Engineering Structures 267 (2022) 114650

Contents lists available at ScienceDirect

Engineering Structures

journal homepage: www.elsevier.com/locate/engstruct

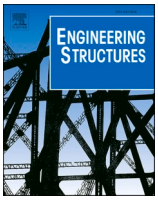

Impact of construction errors on the structural safety of a post-tensioned reinforced concrete bridge

Neryvaldo Galvão [a,*], José C. Matos [a], Rade Hajdin [b], Luís Ferreira [c], Mark G. Stewart [d]

[a] University of Minho, ISISE, Civil Engineering Department, Guimarães, Portugal
[b] Faculty of Civil Engineering, University of Belgrade, Belgrade, Serbia
[c] Faculty of Engineering, University of Porto, Porto, Portugal
[d] The University of Newcastle, Centre for Infrastructure Performance and Reliability, Newcastle, Australia

ARTICLE INFO

Keywords:
Construction errors
Structural safety
Human errors
Bridge collapses
Reliability of structures
Surrogate models
Robustness
Non-linear analysis
Reinforced concrete
Railway bridges

ABSTRACT

The ageing of bridge stock in developed countries worldwide and the increasing number of recorded bridge collapses have underlined the need for more sophisticated and comprehensive assessment procedures concerning the safety and serviceability of structures. In many recent failures, construction errors or deficiencies have contributed to the unfortunate outcome either by depleting the safety margin or speeding up the deterioration rate of structures. This research aims to quantify the impact of construction errors on the structural safety of a bridge considering corresponding models available in the literature that probabilistically characterise the occurrence rate and severity of some of these errors. The nominal probability of failure of structures, neglecting construction errors, is typically computed in numerous works in the literature. Therefore, the novelty of this paper lies in the consideration of an additional source of uncertainty (i.e., construction errors) combined with sophisticated numerical methods leading to a more refined estimation of the probability of failure of structures. Accordingly, some benchmark results focussing on error-free and error-included scenarios are established, providing useful information to close the gap between the nominal and the actual probability of failure of a railway bridge.

1. Introduction

According to current standards [1,2], recently designed and constructed structures should be accompanied by comprehensive as-built or birth certificate documentation. Such documents should include inspection results of the construction process, performed quality control measures, verified design assumptions, and adopted construction techniques, among other relevant information for regular maintenance not available on the design reports or blueprints [3]. Throughout the sixties and the seventies, a period of mass construction, quality control requirements were less demanding than nowadays. That was also a time when digitalisation was in its infancy and available for very few, if any, in the construction industry, making access to this information tedious or even impossible. Regarding the quality assurance throughout the lifespan of the structure, the absence of this information (i.e., as-built, birth certificate reports and documented deviations from design) adds further uncertainties. Such additional sources of uncertainty are likely to lead to unrealistic conventional safety and serviceability reliability assessment. Conventional reliability assessment as defined here doesn't explicitly consider construction errors as a source of uncertainty. Furthermore, the initial margin of safety of such structures has likely suffered some decline due to deterioration and/or load increase since many of these structures already operate in the second half of their designed service life, becoming more sensitive to hidden defects. It is of no relevance whether these defects remained undetected or detected, but the corresponding documentation is lost [4–6].

Bridge collapses typically arouse the interest of engineers and researchers since they offer a unique opportunity to investigate the causes of the collapse, determine the underlying triggering event and gain new insights into structural behaviour. Several databases and meticulous investigations on bridge collapses and their consequences are available today [7,8]. Depending on the source, construction errors during the construction phase are responsible, at least to some degree, for 6–17% of the overall bridge collapses [9–13]. This percentage depends on the

* Corresponding authors.
E-mail addresses: neryvaldo.galvao17@live.com (N. Galvão), jmatos@civil.uminho.pt (J.C. Matos), rade.hajdin@grf.bg.ac.rs (R. Hajdin), lferreir@fe.up.pt (L. Ferreira), mark.stewart@newcastle.edu.au (M.G. Stewart).

https://doi.org/10.1016/j.engstruct.2022.114650
Received 5 April 2022; Received in revised form 23 June 2022; Accepted 4 July 2022
Available online 15 July 2022

considered definition of human errors [14]. While the contribution of construction errors in the overall collapse of bridges has been roughly estimated, their impact on the structural safety reduction of still-standing structures has not been thoroughly investigated. As such, this paper aims the introduction of construction error models in the reliability assessment of bridges.

Regarding the collapse of the Polcevera viaduct (a.k.a Morandi bridge), whose cause is still under investigation, Calvi et al. [15,16] suggest that the failure of one of the four stays attached to the collapsed pylon is the probable cause of the collapse. It seems, however, that the stay's failure is caused by advanced local corrosion of the tendons enabled by the poor grouting on the cables. Thus, an initial construction error and insufficient quality control during construction might have played a role in the bridge's collapse. A more overwhelming contribution of construction errors to the collapse of bridges was recently reported by Pujol et al. [17]. The insufficient prestressing of the main transversal girder and placement of the main reinforcement of the pylon diaphragm in the wrong direction led to the failure of a reinforced concrete cable-stayed bridge during its construction. Deviations from the initial design during the construction phase have also been reported to contribute to the collapse of the Xiaoshan ramp bridge [18].

The need for quality assurance to avoid, identify, and mitigate the consequences of design and construction errors is a well-known requirement within the engineering community and design standards [19]. In design standards, a sufficiently low failure rate as a basis for design checks is assumed, considering unavoidable uncertainties in the design and construction process [2,13,14]. This failure rate is called the nominal failure rate, and the unavoidable uncertainties can be regarded as acceptable deviations. If these deviations were the only ones, the actual failure rate would be the same as the nominal failure rate. However, this is not the case due to human errors. Human error is defined here as any procurement, design, construction and operation errors (i.e., unacceptable deviations) that do not exceed the currently available engineering knowledge and have taken place due to poor work conditions, lack of knowledge, negligence and miscommunication, greed, calculation errors, time and budget constraints, inadequate construction methods and lack of surveillance [14].

Consequently, this paper seeks to consider construction errors in the reliability assessment of a post-tensioned reinforced concrete railway bridge. The outcomes of this paper should help establish some results relevant for possible consideration of construction errors in the definition of partial safety factors and future revisions of design and assessment codes.

2. Construction error models – A short review

The discrepancy between the actual and the nominal failure rate is attributed to human errors [2,20] and actions that are not, or not with sufficient intensity, covered by the codes of practice. However, in the nuclear power plant industry, when safety is concerned, human errors are explicitly considered through a well-established human reliability analysis (HRA) procedure supported by event tree techniques and Monte-Carlo simulation. The HRA allows the modelling of a process by subdividing it into consecutive macro and micro tasks providing the ability to model errors in the performance of a task (i.e., error of commission) or model the consequence of non-performance of a task (i.e., error of omission) [21].

A construction error is described within this work as a deviation of a certain structural parameter, from its design value, beyond the acceptable tolerances assumed by standards. Stewart [21,22] developed an HRA event tree seeking to model construction errors' influence on the failure probability of a typical reinforced concrete beam. The HRA model incorporated tasks directly related to the flexural strength of a beam, such as the (a) longitudinal reinforcement area, (b) effective depth of the tensile reinforcement, (c) beam width and (d) quality of the concrete mix. Considering general guidelines provided by Swain and Guttman [23] and experts' opinions collected in carefully elaborated surveys, the probabilistic appraisal of human error probabilities (HEP) and error magnitudes were possible (see Table 1). Different HEPs are provided (i.e., before and after inspection) based on the assumption that after the inspection of finished construction works, leading to the identification of errors, corrective measures are put in place to eliminate such errors.

Design errors are also relevant sources of uncertainty addressed by Stewart and Melchers [24–27]. Stewart [25] investigated construction and design errors' impact on structural safety reduction and concluded that construction errors were more detrimental to structural safety reduction. Nonetheless, this might not be the case for specific structures or situations. Either way, they are both relevant and should be treated as such. However, the focus of this work is construction errors.

2.1. Human error probability

The HEP is defined by the number of times the error has been observed, provided a total number of performed inspections. Within this paper, one must highlight that the provided HEP models are exclusively limited to the rate of occurrence of construction errors. According to Swain and Guttman [23], a lognormal probabilistic distribution function (PDF) should be used to model HEP, mainly because tasks performed by experienced individuals are expected to accumulate error rates at the lower error end of a distribution, i.e., close to zero; thus, skewing the density function towards zero. The lognormal PDF is chosen in HRA to model operator errors in nuclear power plants.

For the definition of any PDF, a mean value and a measure of the dispersion of the random variable (i.e., variance or standard deviation) must be proposed. The HEP dispersion is a consequence of different personal skills and traits, the work environment, the task itself, and many other factors that might affect the performance of a task. Consequently, Stewart [21,25] proposed the median estimate parameter based on expert judgments collected through a survey disseminated to construction experts and the dispersion parameter set according to guidelines for operator tasks in the nuclear power plants industry. Such parameters are presented in Table 1, where, $\widetilde{m}_0$ is the median and EF_0 is an error factor used to compute the standard deviation σ_0 of the HEP distribution through Eq. (1). The EF_0 is the square root of the ratio between the 90th and 10th percentile values of the PDF of the HEP. In other words, it is a measure that allows one to specify the dispersion of the bounds of a distribution.

$$\sigma_0 = \frac{ln(EF_0)}{1.2817} \tag{1}$$

The HEP PDFs of selected construction errors are given in Fig. 1a. For each error, HEPs before and after the inspection is provided. The

Table 1
Parameter for human performance models (construction) [21].

Error type	Before Inspection		After Inspection		λ_{BE}	λ_{UB}
	$\widetilde{m}_0$	EF_0	$\widetilde{m}_i$	EF_i		
E1 Reduced area of reinforcement	0.0218	5	3.73E-4	10	−14.30	−82.22
E2 Increased area of reinforcement	0.0114	5	1.95E-4	10	15.16	69.22
E3 Decreased effective depth	0.0296	5	5.06E-4	10	−7.10	−21.14
E4 Increased effective depth	0.0188	5	3.21E-4	10	6.27	16.60
E5 Decreased beam width	0.0081	3	1.39E-4	10	−5.24	−14.54
E6 Increases beam width	0.0083	3	1.42E-4	10	5.22	16.52
E7 Inadequate concrete mix	0.0049	3	0.0049	3	−9.58	−38.1

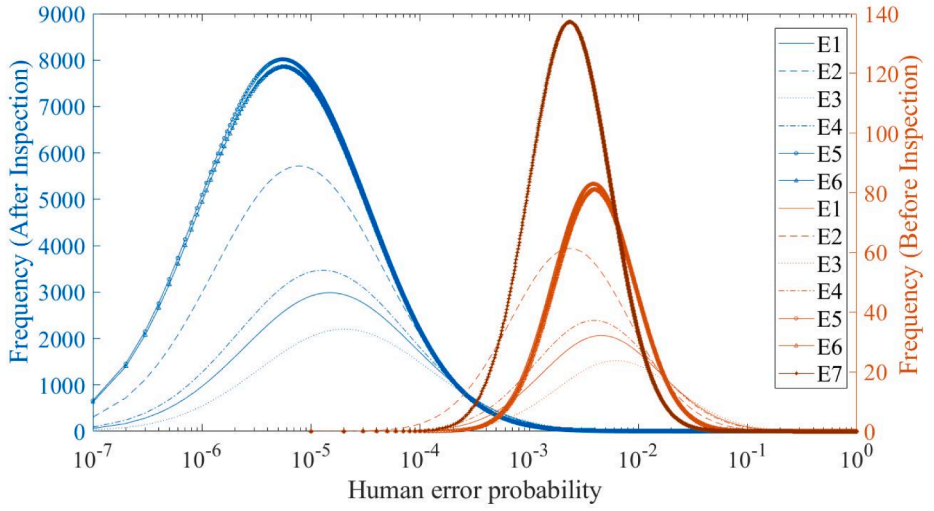

Fig. 1. (a)PDFs of HEPs before inspection (orange) and after inspection (blue); (b) PDFs of error magnitudes.

influence of inspection and subsequent implementation of corrective measures in the HEP PDFs is evident, with the mean value decreasing by several orders of magnitude for the same error despite the increase in the dispersion of the distribution. The previous statement is true except for E7 (i.e., inadequate concrete mix) since the HEP is maintained after the inspection. Such exception is mainly because visual inspections are considered to take place, making unfeasible the assessment of the compliance of the concrete strength.

2.2. Error magnitude

The error magnitude m_e is here defined as the percentage deviation from the designed outcome of a construction process according to Eq. (2). In short, m_e is the severity of the error:

$$m_e = \frac{z - z_m}{z_m} \times 100\% \tag{2}$$

where z_m is the designed outcome, and z is the measured or estimated actual outcome. Two types of error are considered to model the error magnitude: an error of commission and an error of omission. An error of commission is a deviation with the error magnitude ranging from 0% to 99% from the designed outcome. The error of omission is the failure to execute a process (i.e., $m_e = -100\%$). For instance, if a complete layer of reinforcement is missing, an error of omission has taken place. On the other hand, if a few bars of reinforcement are missing in a deployed layer of reinforcement, an error of commission has taken place. Simply put, an error of commission is the wrongful performance of a task, while an error of omission is the failure to perform a task. In addition, errors can be detrimental or beneficial to the structure's resistance; thus, both positive and negative percentage deviations must be considered.

An error of omission might be more frequent for some types of error than others; nevertheless, one can state with reasonable confidence that they are less frequent and likely to be revealed during the inspection process and corrected afterwards. The proposed PDF for the error magnitude is also a lognormal distribution defined according to the provided median estimate λ_{BE} and the 90th percentile upper bound estimate λ_{UB} of the PDF (see Table 1). The standard deviation of the error magnitude PDF σ_{me} is computed through Eq. (3).

$$\sigma_{me} = \frac{ln\left(\frac{\lambda_{UB}}{\lambda_{BE}}\right)}{1.2817} \tag{3}$$

The lognormal distributions obtained because of the detrimental and beneficial errors are displayed in Fig. 1b. The possible range of deviations for beneficial errors can exceed 100%; however, this is very unlikely. On the other hand, error magnitudes for detrimental errors are limited to error magnitudes not greater than −100% (i.e., error of omission) [21,22].

2.3. HRA event tree

Stewart [21] proposed an event tree (see Fig. 2) to combine the realisations of the HEPs and error magnitudes according to their respective PDFs described in 2.1 and 2.2. Later on, Epaarachchi and Stewart [28] also considered such an event tree to discuss construction errors' impact on multi-story reinforced concrete buildings. The proposed event tree allows the simulation of construction outcomes within the expected range of deviation allowed by construction tolerances and the simulation of construction outcomes outside of such acceptable ranges of deviation (i.e., detrimental, and beneficial errors).

Error-free and error-included realisations are allowed by the event tree, and their rate of occurrence is dependent on the HEP PDFs considered and the realisation of a random number (RN_i) with a uniform distribution. Simply stated, the rate of occurrence of a detrimental error in the overall number of generated samples is given by the number of times the realisations of RN_i is lower than the realisation of the considered HEP. The size of the deviation from the nominal value X_{nom} (i.e., mean value) is given by the detrimental and beneficial error magnitude PDF (i.e., $EM_{i,d}$ or $EM_{i,b}$, respectively). Furthermore, it is important to highlight that the realisations of HEPs, EMs and RN_i, are all independently generated according to their respective PDF. Accordingly, the probability of failure of the structure is computed considering these main two branches of the event tree, namely, error-free and error-included realisations, where the error rate is given by the number of times the realisation of RN_i, with a uniform PDF between 0 and 1, is lower than $HEP_{i,d}$ and $HEP_{i,d} + HEP_{i,b}$ (see Fig. 2). The i, d and c indexes are respectively the i^{th} number from the sample vector obtained from the PDFs of the d^{th} detrimental error (i.e., E1, E3, E5 and E7) and b^{th} beneficial error (i.e., E2, E4 and E6).

For illustration purposes, the influence of the E7 models (i.e., inadequate concrete mix) in the PDF of the concrete compressive strength is presented in Fig. 2. One should note that the PDF is truncated for a probability density of 1×10^{-3}, aiming to emphasise the main differences between the tail of the error-free and the error-included PDF. Further elaboration on the HRA event tree is presented in 6.

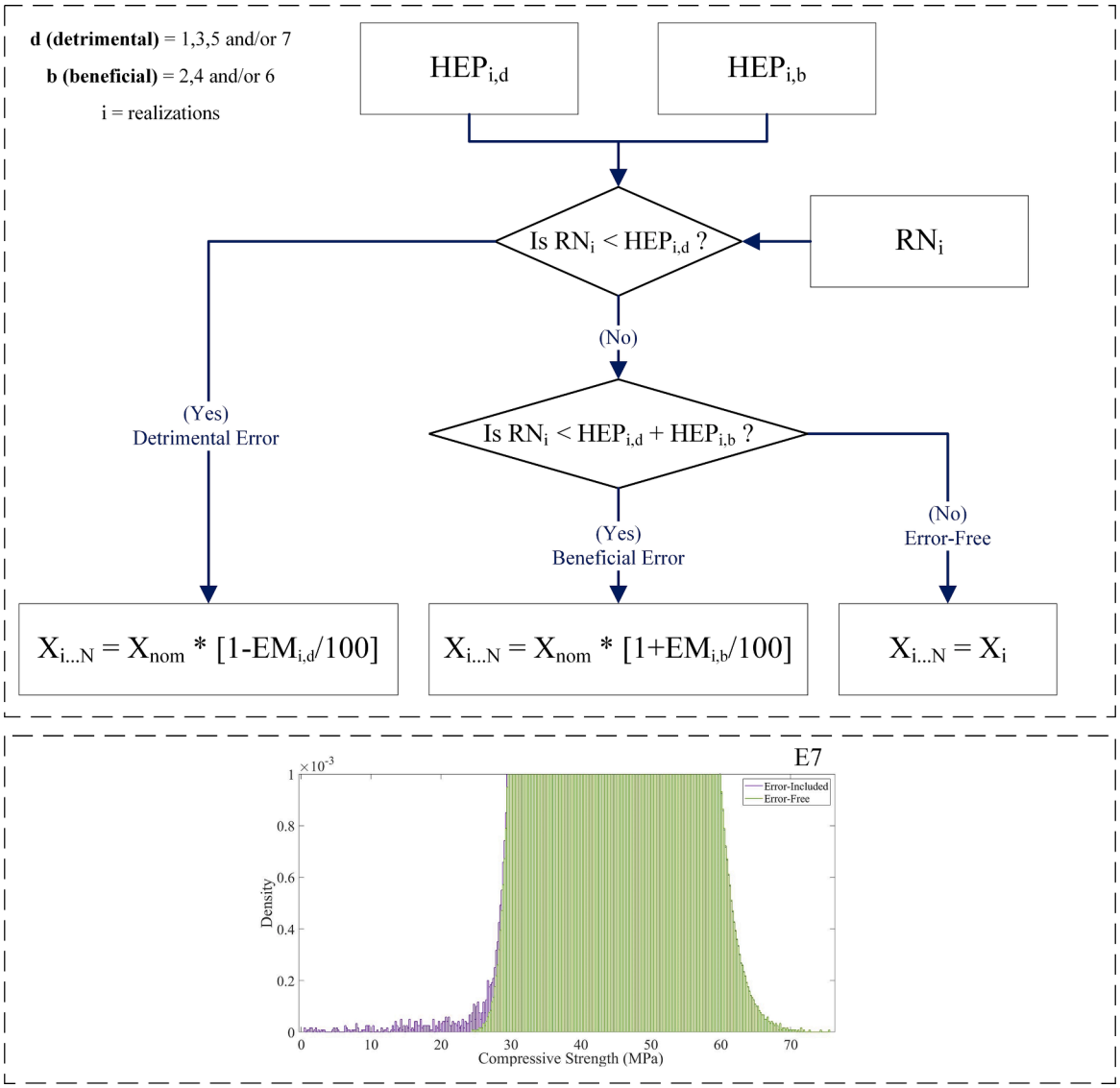

Fig. 2. HRA Event tree with some output results.

3. Surrogate-based reliability analysis

Reliability analysis using finite element models (FEM) can be computationally expensive, particularly for simulation-based approaches where each run requires full FEM analysis. Therefore, surrogate models have been extensively used because they allow the replacement of an expensive numerical model (i.e., FEM) for a far less computationally demanding model that can predict the output of interest with sufficient accuracy for reliability analysis. Surrogate models are the result of supervised machine learning techniques that map the relationship between a set of input and output parameters. Considering that $G(X)$ is the performance function set to assess the violation of a limit state equation (i.e., $G(X) \leq 0$), the probability of failure can be computed as follows in Eq. (4):

$$P_f = P[G(X) \leq 0] = \int_{G(X)\leq 0} f_X(X)dx \tag{4}$$

Where $f_X(X)$ is the joint density function of the random variables X considered to estimate the resistance and loading of the system. Thus, if the safe and the failure domain can be easily drawn by verifying the performance function $G(X)$, the failure probability can be estimated. Accordingly, for a less expensive approximation of $G(X)$ surrogate models have been introduced.

Several surrogate modelling techniques can be found in the literature, e.g., kriging, polynomial chaos expansion, neural networks, support vector machine, and response surface, among others [29–31]. Nevertheless, for the current investigation, a kriging-based surrogate model was selected to approximate the performance function of the case study under assessment. Kriging is a controlled learning procedure that seeks to solve a stochastic problem where the output of interest is the realisation of a gaussian process, i.e., a stochastic process where a finite combination of its random variables has a normal PDF. The prediction given by the surrogate model for the experimental design samples (i.e., initial samples used to train the surrogate) interpolates the exactly known solution (i.e., the observation from the true numerical model). A kriging-based surrogate model is generally described by the following Eq. (5) [32,33]:

$$M^k(X) = \rho^T f(X) + \sigma^2 Z(X, w) \tag{5}$$

Where, $M^k(X)$ is the model output given by the realisation of a gaussian process indexed by the random variable X, ρ^T is a vector of regression coefficients of possible arbitrary base functions $f(X)$ (e.g., polynomial, quadratic, among others). The first term of the equation provides the deterministic approximation of the output of interest in the vicinity of its mean value. $Z(X, w)$ and σ^2, are the zero-mean and unit-variance stochastic Gaussian process and the constant that represents the variance of the gaussian process, respectively.

Notwithstanding the increased efficiency afforded by a surrogate model, a surrogate-based reliability analysis can be further improved by an active learning technique that allows the approximation of the performance function in the vicinity of the limit state equation $G(X) = 0$ using a learning function in a process known as the enrichment procedure [33–35]. Such a procedure is used in a loop until a convergence criterion is satisfied. The stability of the reliability index (i.e., the convergence criteria) is verified in Eq. (6) as follows:

$$\frac{|\beta^j - \beta^{j-1}|}{\beta^j} \leq \epsilon_\beta \tag{6}$$

Where β^j and β^{j-1} are the reliability index of the jth and its preceding iteration, respectively. The threshold value ϵ_β considered in this work is 0.02.

To estimate the probability of failure the subset simulation is chosen. The subset simulation technique is an efficient and robust simulation-based technique that allows the estimation of very low probabilities of failures. Such sampling technique is supported by the definition of a sequence of failure domains ($D_1 \supset D_2 \supset D_3 \ldots D_i$) where the final intersection of all the failure domains will equal the actual probability of failure of the numerical problem ($D_f = \bigcap_{k=1}^{i} D_k$). A group of decreasing threshold values $t_1 > t_2 > t_3 \cdots t_i = 0$ determines a set of different limit state equations (i.e., $G(X) \leq t_i$) that define the domains (D_i) in such a way that the probability of each event related to D_i (i.e., $P(D_i)$) is close to a pre-established probability P_0 (i.e., $P(D_i) \approx P_0$ where $0 < P_0 \leq 0.5$). Henceforth, the probability of failure of a defined sequence of failure domains is estimated through the multiplicand of conditional probabilities ($D_{j+1}|D_j$), according to Eq. (7) [36,37]:

$$P_f = P\left(\bigcap_{k=1}^{i} D_k\right) = P(D_1)\prod_{j=1}^{i-1} P(D_{j+1}|D_j) \tag{7}$$

For evaluation of the quality of the surrogate model in the approximation of the expensive numerical model, the leave-one-output cross-validation error (ϵ_{LOO}) given in Eq. (8) is used as the error measure.

$$\epsilon_{LOO} = \frac{1}{N}\left(\frac{\sum_{i=1}^{N}[G(x_i) - Y_{val}(x_i)]}{Var[G]}\right) \tag{8}$$

where $G(x_i)$ is the output of the accurate model (i.e., FEM) and $Y_{val}(x_i)$ is the surrogate model output for the realisations x_i of the random variables, both computed based on a validation sample. $Var(G)$ is the variance of all the known values of $G(x_i)$.

4. Case study

4.1. Bridge description

A post-tensioned reinforced concrete railway bridge is introduced to investigate the construction errors' impact on structural safety. The case study is a three-span post-tensioned reinforced concrete overpass of 52 m in length constructed in Pinheiro, Portugal, in 2010. The outward spans are 15 m, while the middle span has 22 m in length (see Fig. 3a). Two solid V ribs attached to a concrete slab shape the superstructure, each supporting a rail track. The ribs are 2 m and 2.6 m in width, in their bottom and top sections, respectively, attached to a standard concrete slab of 12.9 m in width and 0.35 m thick (see Fig. 3b). The superstructure has a total height of 1.5 m, and the ribs are spaced by 5.4 m. The superstructure is monolithically connected to two piers with 9.73 m in height, and it is supported over the abutments by elastomeric bearing devices through transversal girders. The piers foundation contains piles of more than 31 *m*, connected by rigid pile caps that support the piers. The piers' cross-section is displayed in Fig. 3c. The overpass was designed according to the Portuguese regulation for reinforced and prestressed concrete structures (REBAP) and the regulation for safety and load of structures (RSA), using a static live load model equivalent to the load model 71 (LM71) of Eurocode 1 [38] and considering 40 *mm* minimum concrete cover given the exposure conditions.

The bridge superstructure was built using a C35/45 concrete, while the piers were executed with a C30/37 concrete. The structure was reinforced by S500-A steel reinforcement and post-tensioned by a low relaxation (i.e., class 2) bonded reinforcement Y 1860 S22 15 mm. All its elements were cast in situ, using falseworks as temporary supports. The superstructure is prestressed by six cables per rib in its length, with varying heights (see Fig. 3d). Each cable is made of 22 strands of 1.5 cm^2 of area. The expected immediate and time-dependent losses of the applied post-tensioning forces were estimated to be between 22% and 27%. The estimated long-term post-tensioning forces are available in Fig. 3d.

4.2. Numerical modelling

For non-linear structural analysis purposes, half of the bridge is modelled using two-dimensional FEM in DIANA FEA software [40–42].

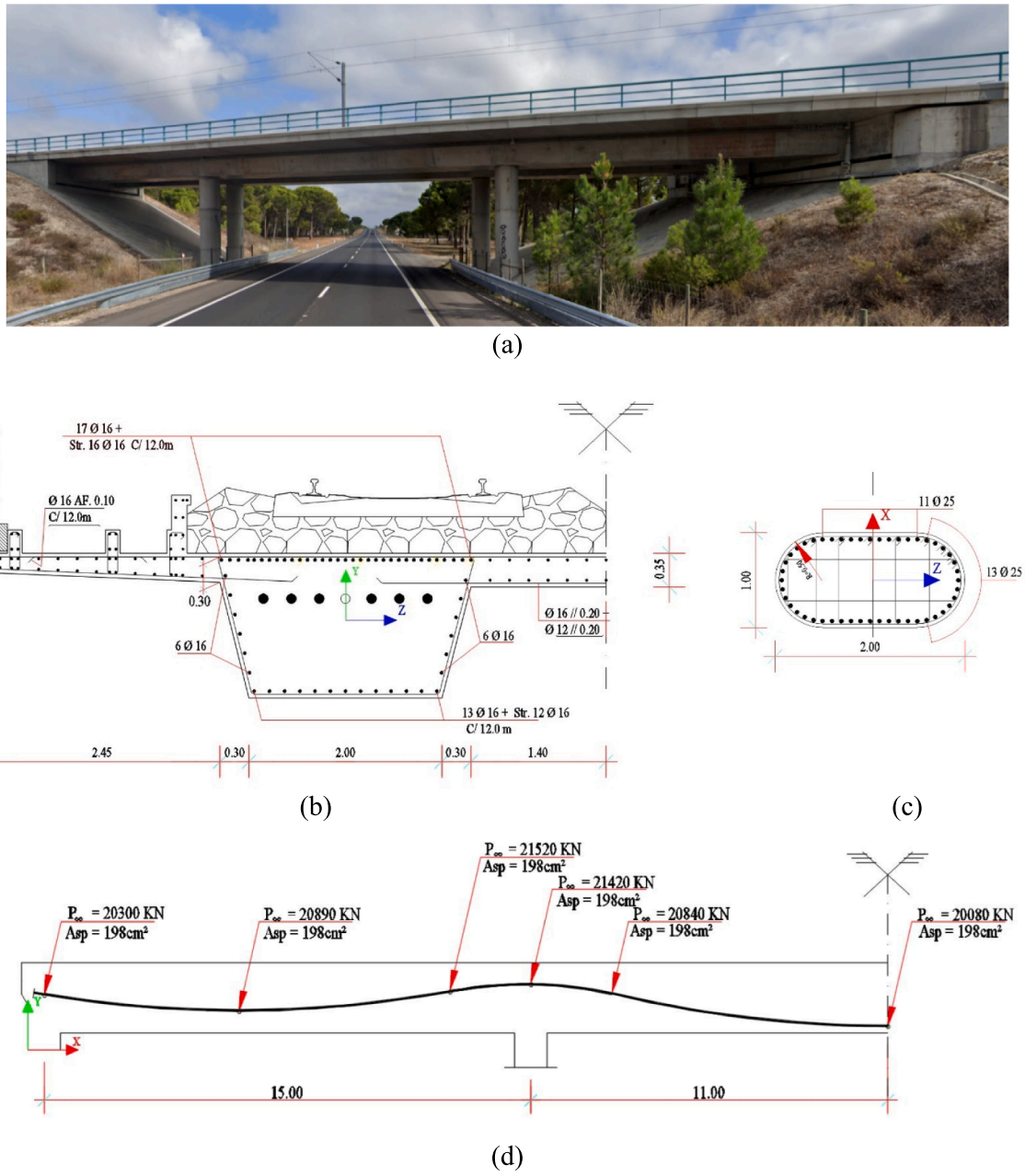

Fig. 3. Case study; (a) picture (google maps view); (b) reinforced superstructure cross-section; (c) piers cross-section; and (d) prestressing cables layout and their minimum expected prestressing forces obtained from blueprints ().
Adapted from:[39]

The model aims to characterise the maximum carrying capacity of the structural system (i.e., ultimate limit state (ULS)) when bending is concerned. The superstructure and piers were modelled by a fully numerically integrated (in its axis and cross-section) class III-Mindlin-Reissner beam element of 0.25 *m,* with three nodes and three degrees of freedom per node (i.e., u_x, u_y and $\varnothing_z$). Equivalent cross-sections were used to model the superstructure cross-section and the piers. The superstructure was modelled with seven layers (see Fig. 4a), each with five integration points in its height, while the piers are modelled with a simpler cross-section. For integration purposes, the composite Simpson rule was employed.

A fixed total strain-based crack model was considered to depict the non-linear behaviour of concrete, as recommended by Hendriks et al. [43]. The concrete was modelled by the constitutive model in Fig. 4b, while the conventional and post-tensioned reinforcement behaviour was modelled by the constitutive model in Fig. 4c. For post-tensioning of the superstructure, the prestressing reinforcements were considered initially unbonded as the superstructure was being loaded by its self-weight and the post-tensioning forces, followed by a bonded phase when applying the remaining permanent and live load. The material mechanical properties used for the preliminary deterministic structural analysis discussed in 4.3 are provided in Table 2 and Table 3.

The self-weight of the reinforced concrete structure was estimated considering 25 kN/m^3 of weight, leading to a total self-weight of 116.3 kN/m. The total remaining permanent load comprising, namely; (i) the ballast, (ii) sleepers, (iii) rails, (iv) precast covers, (v) precast slabs, (vi) ballast protection, (vii) cornices, (viii) guardrails and (ix) cables' gallery filling, was approximated around 72.8 kN/m. The rail traffic static vertical loads were modelled according to the LM71 [38]. Nevertheless, for the structural analysis results presented in 4.3, mean values of LM71

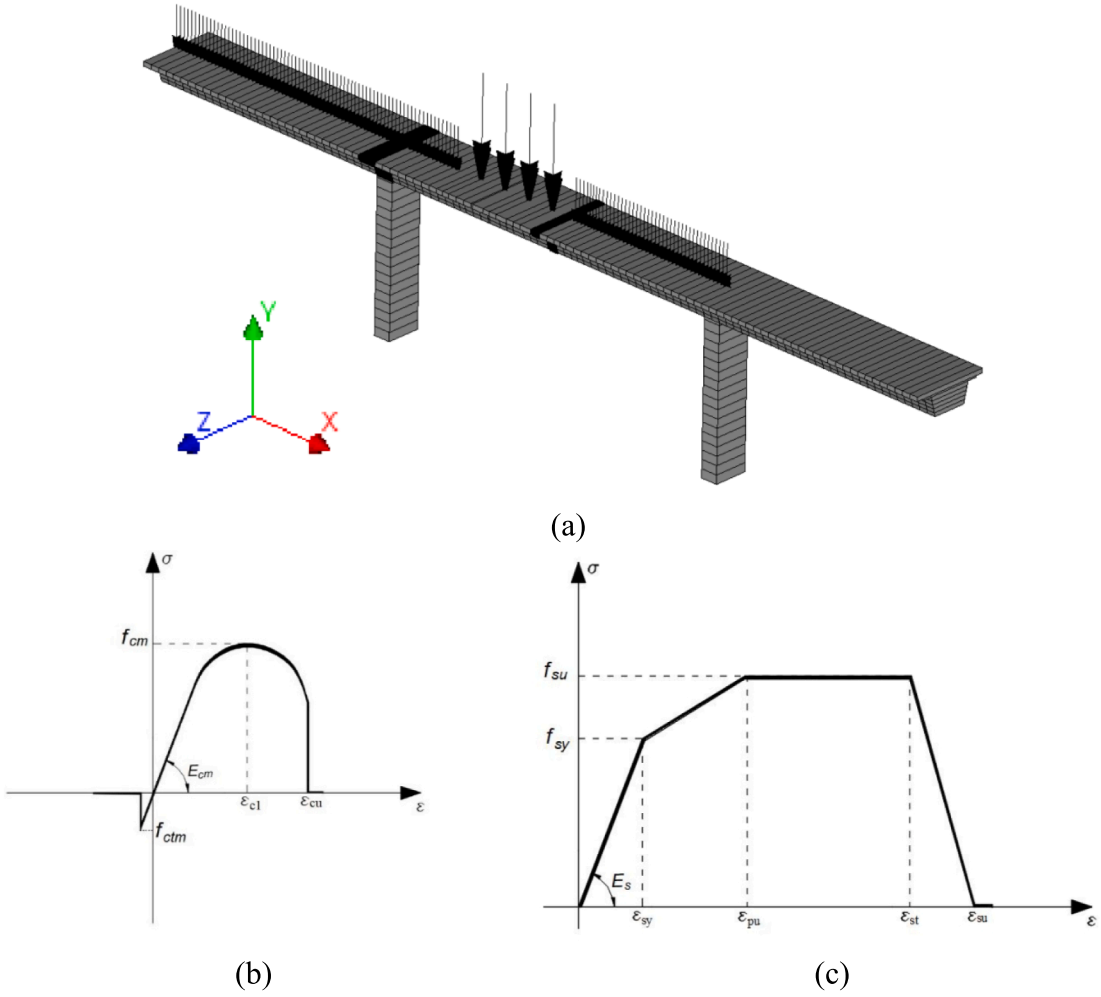

Fig. 4. (a) Numerical model extruded geometry; (b) concrete constitutive model and (c) conventional and post-tensioning reinforcement constitutive model.

Table 2
Concrete mechanical properties.

	E_{cm} (GPa)	f_{ctm} (MPa)	f_{cm} (MPa)	ε_{c1} (‰)	ε_{cu} (‰)
C30/37	33	2.9	38	2.2	3.5
C35/45	34	3.2	43	2.3	3.5

Table 3
Reinforcement mechanical properties.

	S 500-A	Y 1860 S22 15 mm
ε_{sy}	0.0028	0.00822
ε_{pu}	0.025	0.02
ε_{st}	0.05	0.05
ε_{su}	0.1	0.1
E_s (GPa)	200	200
f_{sy} (MPa)	560.0	1644.0
f_{pu} (MPa)	580.0	1934.0

are considered, bearing in mind that the provided characteristic values equal the 98th percentile of a Gumbel PDF with a coefficient of variation (CoV) of 10%, considering a 50-year reference period (see Table 5).

The case study was designed and assessed considering an alpha factor equal to 1.0. The dynamic amplification effects caused by the speed of the moving load, irregularities of the track, vehicle imperfections, spacing of axle loads, and suspension characteristics of the vehicles, among other reasons, were considered through a dynamic amplification factor of 1.21, assuming a track under standard maintenance [38]. Provided the adequate structural system influence line, the LM71 was positioned to maximise its effects on the superstructure cross-section over one of the piers (see Fig. 4a). Such a cross-section was proven to be the critical one when longitudinal bending is concerned.

4.3. Non-linear structural analysis

For non-linear structural analysis, an incremental-iterative loading procedure based on the Modified Newton Raphson iteration scheme and force control incremental procedure was implemented using energy and force norm as convergence criteria. Accordingly, the maximum carrying capacity of the structural system when longitudinal bending is concerned, and the failure is characterised by the material's strength (i.e., ULS: STR), was estimated to be approximately 6.7 times the mean value of LM71, according to Fig. 5a. The Fig. 5a displays the load–displacement curve of the middle span cross-section highlighted in Fig. 4a. Further analysis considering the 5% quantile values and design values (using resistance partial safety factors of Eurocode 2 [44]) of the concrete compressive strength, and conventional and post-tensioning reinforcement yielding strength, was also performed, aiming to assess the structural system carrying capacity for such deviations. The remaining parameters were kept with their mean values. In summary, the data shows an 8.96% and 24.78% reduction in the system carrying capacity for the 5% quantile and the design values, respectively.

The maximum carrying capacity is attained after reinforcement yielding and bending moment redistribution due to concrete crushing in

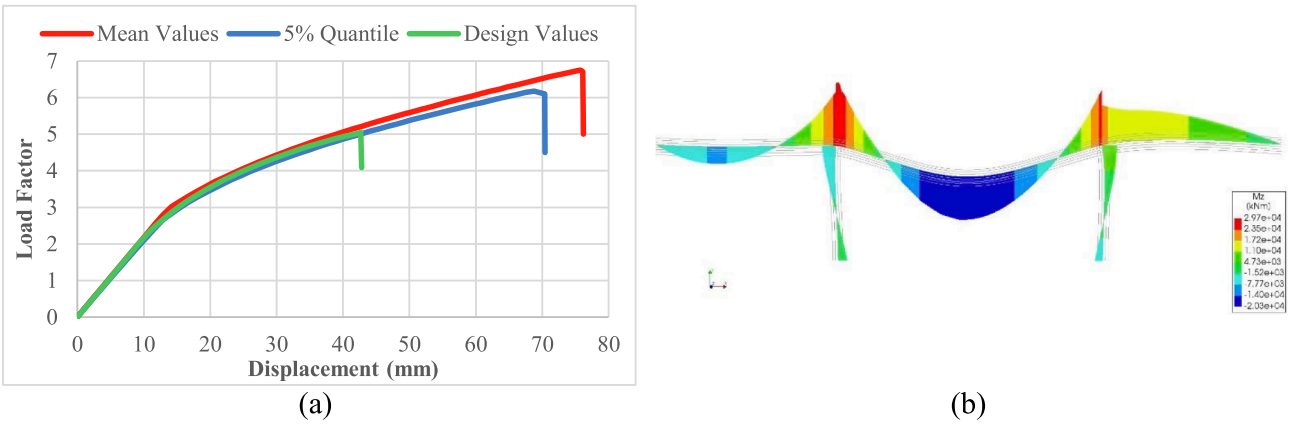

Fig. 5. (a) Load-displacement curve (b) bending moment diagram distribution for maximum load factor;

the lowest fibre of the superstructure cross-section over the pier when the concrete reaches its ultimate compressive strain of 3.5‰. The maximum bending moment capacity of the superstructure cross-section over the piers is estimated to be 28,528 kNm (see Fig. 5b).

5. Reliability assessment

5.1. Resistance and loading uncertainties

Structural safety is often assessed using structural reliability analysis to evaluate failure probability given uncertainties in the assumption of the loading and resistance. However, human error is also an important source of uncertainty, neglected too often in such analysis, despite being addressed through quality control measures. In this section, a conventional structural reliability assessment (i.e., neglecting construction errors) is performed. In the subsequent section, construction errors probabilistically characterised in section 2 are introduced as an additional source of uncertainty through an HRA event tree in a more comprehensive reliability analysis procedure. Based on the literature [45–53], stochastic models for resistance and loading used in the reliability analysis are given in Table 4 and Table 5, respectively.

In Europe, bridges designed according to the Eurocode 2 [54] should

Table 5
Probabilistic characterisation of permanent loads, live load and load model uncertainty random variable.

ID	Random Variables	Notation	Mean Values	CoV	PDF	Reference
1	Self-weight load[1,2]	DL	25.8 kN/m^3	7.1%	Normal	[45]
2	Additional load[1,3]	AL	72.8 kN/m	11%	Normal	[45]
3	Live load model uncertainty	θ_S	1.0	15%	Normal	[51]
4	Lifetime (50-year peak) Live load model 71[4,5]	LM71	198.5 kN (63.2 kN/m)	10%	Gumbel	[52,53]

[1] Model uncertainty included.
[2] Correlated with slab thickness ($\rho = 0.5$).
[3] Sleepers, rails, railings, etc.
[4] Characteristic value provided by EC corresponded to the 98th percentile.
[5] 50-year reference period.

Table 4
Probabilistic characterisation of materials, geometries and model uncertainty random variables.

ID	Random Variables		Notation	Mean Values	CoV	PDF	Reference
1	C35/45	Compressive strength	f_{cm}	43 MPa	12%	Lognormal	[45]
2		Tensile strength[1]	f_{ctm}	3.2 MPa	20%	Lognormal	[45,46]
3		Modulus of elasticity[2]	E_{cm}	34 GPa	8%	Normal	[46]
4		Slab thickness	t	25.5 cm	3.5%	Normal	[47]
5	S500A	Yielding stress	f_{sy}	560 MPa	5.4%	Lognormal	[48]
6		Ultimate Strength[3]	f_{su}	580 MPa	6.9%	Lognormal	[48]
7		Area[4,5]	A_s	–	2%	Normal	[48]
8		Effective Depth[6]	d_s^+	Nom.*1.4	15%	Lognormal	[47]
				Nom.*1.0	3.3%		[49]
9	S1670/1860	Yielding stress	f_{py}	1644. MPa	2.5%	Normal	[48]
10		Ultimate Strength[7]	f_{pu}	1934 MPa	2.5%	Normal	[48]
11		Prestressing force (t = ∞)[8]	F_∞	20300–21520 kN	9.0%	Normal	[48]
12		Area[7]	A_p	–	1.2%	Normal	[47]
13	Resistance model uncertainty		θ_R	1.00	17%	Lognormal	[50]

[1] $f_{cm} - f_{ctm} \rightarrow$ Correlation coefficient $(\rho) = 0.7$.
[2] $f_{cm} - E_{cm} \rightarrow \rho = 0.9$.
[3] $f_{sy} - f_{su} \rightarrow \rho = 0.85$.
[4] $A_s - f_{sy} \rightarrow \rho = 0.5$.
[5] $A_s - f_{su} \rightarrow \rho = 0.35$.
[6] The effective depth is measured from the top layer of the bridge superstructure.
[7] The correlations valid for conventional reinforcement properties are also valid for the prestressing reinforcement.
[8] The prestressing force applied to the different tendons are considered fully correlated coefficient.

be executed according to the EN13670 [55] with careful attention to the construction tolerances allowed by the standard and workmanship recommendations. The range of values allowed by the PDF of the random variables and the construction tolerances provided by the standards are reasonable benchmarks that can be used to determine the boundaries between acceptable and unavoidable random variations and construction errors. Nonetheless, the density function associated with the ranges of acceptable random variations must not be neglected.

Using DIANA FEA software in combination with UQLab sampling algorithms [56,57], an initial investigation of the unavoidable uncertainty impact on the maximum carrying capacity of the case study was performed. The variability of the maximum carrying capacity of the structure, measured as a load factor of the mean value of LM71, caused by the stochastic models summarised in Table 4 and Table 5 (apart from the resistance θ_R and live load θ_S model uncertainty as well as live load uncertainty) is displayed in Fig. 6a and Fig. 6b, considering 400 samples generated through the Latin hypercube sampling technique. In summary, the PDF of $R(X)$ in Eq. (9) is roughly estimated by the histogram given in Fig. 6b. The variability of the maximum carrying capacity of the structure, defined by the histogram in Fig. 6b, has a mean value of 6.52 and a standard deviation of 0.28. The 2% and 98 % quantile values of the histogram are 5.89 and 7.02, respectively.

5.2. Safety evaluation

For reliability assessment, the limit state equation $G(X) = 0$ (see Eq. (9)) is defined as the boundaries between the failure and the safe domain necessary for failure probability evaluation. Thus, the safe and the failure domain are defined by $G(X)\rangle 0$ and $G(X) \leq 0$ respectively.

$$G(X) = \theta_R \times R(X) - 1.21 \times S \times \theta_S = 0 \tag{9}$$

Where, $R(X)$ is the load-carrying capacity defined as a factored mean value of LM71 (roughly estimated in Fig. 6b) given a group of random variables (X) selected based on a sensitivity analysis (see [58,59]), θ_R is the resistance model uncertainty, 1.21 is the considered dynamic amplification factor, S is the load parameters that represent the LM71 with a unitary mean value and the same CoV given to LM71, and θ_s is the live load model uncertainty. One should highlight that $R(X)$ represents the remaining load-carrying capacity of the structural system in the presence of permanent loads.

Employing a surrogate-based reliability analysis approach for reliability analysis as described in section 3, by coupling the UQLab [32,34] algorithms for kriging-based surrogate modelling and active learning techniques (based on U learning functions) with DIANA FEA [42] to predict the output of interest $R(X)$, the probability of structural failure, as well as its confidence interval (CI), are estimated. Initially, 30 experimental design samples were generated followed by a 2-point enrichment procedure considered to refine the surrogate model in the vicinity of the limit state function. The enrichment procedure ends when the stopping criteria defined in Eq. (6) is fulfilled for two consecutive steps. Furthermore, the subset simulation technique was used to estimate the lifetime (50 years) probability of structural failure.

The convergence rate in the computation of the failure probability for each incremental evaluation of the FEM or each generated enrichment sample is displayed in Fig. 7. After 118 FEM evaluations, the lifetime probability of structural failure was estimated as $P_f = 3.62 \times 10^{-13}$ with a CoV of 0.046, putting the structural reliability index between 7.16 and 7.19 (see Table 6). The quality of the surrogate model was assessed according to Eq. (8), yielding a leave one output cross-validation error $\epsilon_{Loo} = 3.18 \times 10^{-4}$, which is a reasonable result, according to Blatman and Sudret [60].

The recommended minimum target reliability index for a ULS of structural members of structures belonging to a reliability class 2, considering a 50-year reference period, is 3.8 according to Eurocode 0 [2] and Ghasemi and Nowak [61]. Moreover, according to Sykora et al. [62], a 0.5 increment to the target reliability index was considered since the analysis presented here is performed at the system level. Nonetheless, one should state that this further increment is conservative and further investigation to search for a less conservative target reliability index is recommended.

From the structural reliability assessment point of view, safety is assured ($\beta > \beta_T$) due to the high-reliability index value obtained, which is higher than the target reliability index of $\beta_T = 4.3$. The high-reliability index value is mainly due to the redistribution capability of the structural system in the longitudinal direction.

Despite the relevance of the approach used to estimate the variability of the maximum carrying capacity of the structure (see Fig. 6) as well as the structure reliability index, one must recognise its limitation. The stochastic models introduced in this analysis were fully correlated throughout the numerical model. To overcome this limitation, random fields should be introduced in the analysis. Nonetheless, one cannot stress enough the increase in computational costs that this approach demands. A simplistic approach for considering spatial variability of stochastic models would be to allow the independent realisation of the random variables in the cross-sections highlighted in Fig. 4a. This would mostly require duplication of most of the stochastic models given in Table 4, which of course, comes with additional computational costs.

6. Impact of construction errors

Following the evaluation provided by a conventional framework for reliability assessment (i.e., human errors excluded), the construction

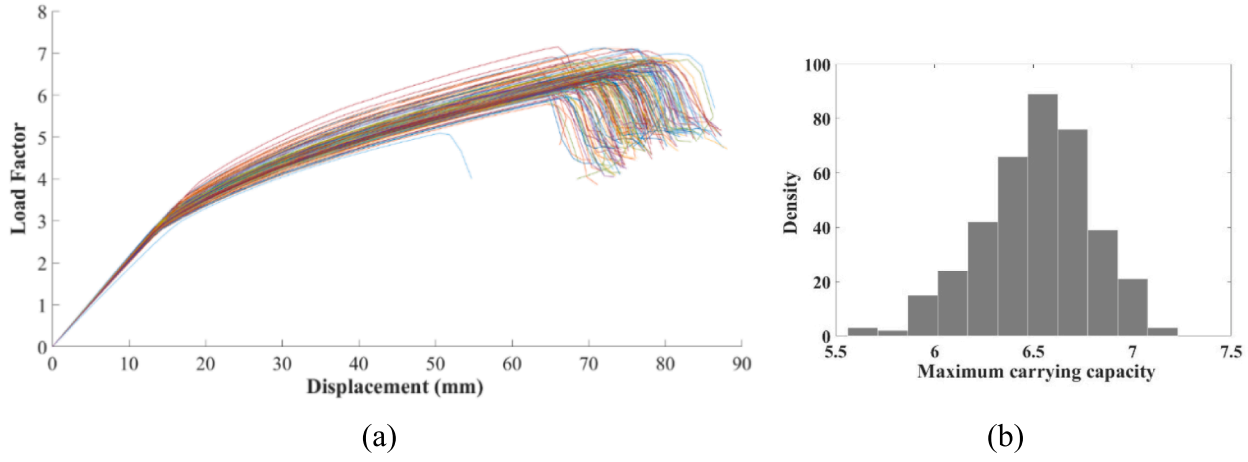

Fig. 6. (a) Load-displacement curve of multiple simulations and (b) histogram of the maximum carrying capacity.

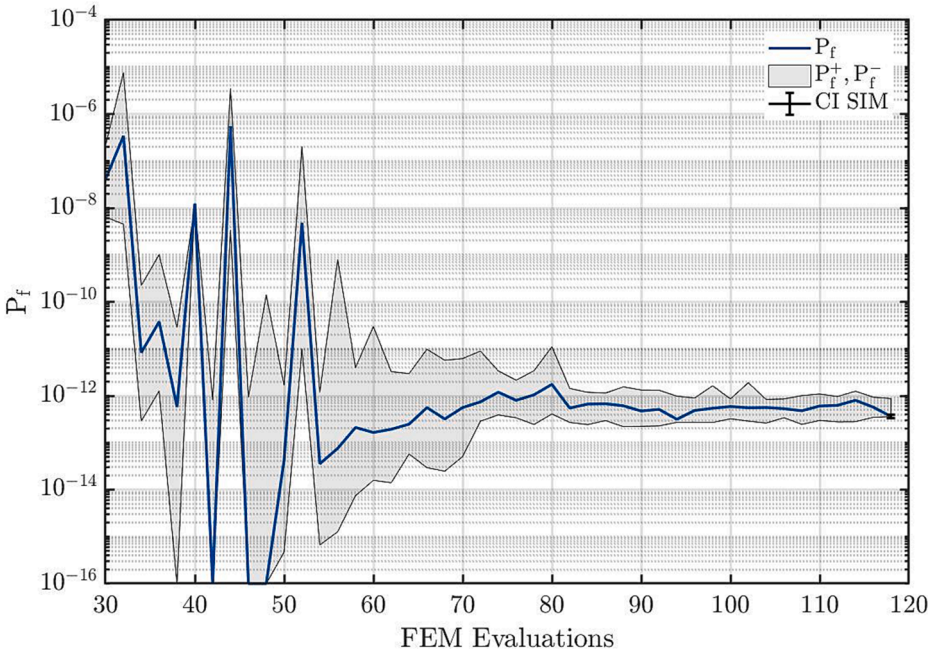

Fig. 7. Probabilistic analysis convergence rate.

Table 6
Probabilistic analysis results.

Method	β [CI]	CoV	P_f [CI]	FEM Evaluations
AK-SS-U	7.17 [7.16 – 7.19]	0.046	3.62×10^{-13} [3.29×10^{-13} – 3.94×10^{-13}]	118

error PDFs introduced in 2 are here considered as an additional source of uncertainty aiming to probabilistically assess the impact of human errors during construction on the structural safety of the post-tensioned reinforced concrete bridge. In a preceding study, Galvão et al. [58] had deterministically evaluated the impact of some construction and design errors on the structural safety of a prestressed reinforced concrete roadway bridge considering error magnitudes. Here, construction errors are modelled as possible occurrences and not as already observed or identified errors.

The analysis performed in this section is summarised as follows; in subsection 6.1 each error, detrimental or beneficial, is independently introduced considering only their respective error magnitude PDF, i.e., disregarding the HEP PDFs (see Table 7). Subsection 6.2 encompass the implementation of the HRA event tree (see Fig. 2) for combinations of detrimental and beneficial errors (e.g., E3 + E4, among others – see Table 8). A sensitivity analysis concerning HEP reduction is performed in 6.3 (see Fig. 8). In 6.4, the HRA event is implemented by combining two or more detrimental errors (e.g., E1 + E7, E1 + E3 + E4, among others – see Table 10). Note that here multiple error occurrences address the possibility of occurrence of multiple errors.

Table 7
Reliability index and failure probability due to the error magnitude PDFs.

Error models	Reliability index (Probability of failure)		
	No bounds	**m_e bounds**	**With bounds**
E1	3.01 (1.31×10^{-03})	0% – 50%	6.13 (4.35×10^{-10})
E2	7.20 (3.07×10^{-13})	–	–
E3	6.97 (1.62×10^{-12})	0% – 50%	7.09 (6.89×10^{-13})
E4	7.08 (7.24×10^{-13})	–	–
E5	4.40 (5.30×10^{-06})	0% – 30%	7.00 (1.27×10^{-12})
E6	7.15 (3.89×10^{-13})	–	–
E7	1.81 (3.54×10^{-02})	0% – 50%	6.72 (9.41×10^{-12})

Table 8
Probability of failure given HRA event tree.

Error models	Reliability index (Probability of failure)	
	After inspection	Before inspection
E1 + E2	4.55 (2.74×10^{-06})	3.86 (5.72×10^{-05})
E3 + E4	7.15 (4.45×10^{-13})	7.15 (4.32×10^{-13})
E5 + E6	5.78 (3.79×10^{-09})	5.29 (6.18×10^{-08})
E7	3.49 (2.52×10^{-04})	3.49 (2.52×10^{-04})

The construction errors models are introduced in the surrogate-based reliability analysis procedure through the HRA event tree proposed by Stewart [21]. In short, for each beneficial, detrimental and combination of detrimental errors, a surrogate model is set to assess the performance function G(X) and subsequently the probability of failure.

Notwithstanding the significant computational cost reduction achieved by the defined surrogates of the FEM, further reduction of the computational costs was necessary. The computational cost reduction to a realistic timeframe was achieved through the vectorisation of the Matlab script used to model the HRA event tree and the script used to invoke UQLab's algorithms for reliability analysis [36]. Vectorisation is a computer programming technique that allows the application of operations or functions to the whole vector or matrix instead of applying them to their individual elements. This allows one to reduce the computational costs (i.e., increase computational speed) of a script in several orders of magnitude (i.e., three to four orders of magnitude) [63].

6.1. *Single error analysis – Error magnitude PDFs only*

The influence of the error magnitude PDFs alone on the structural failure probability was initially assessed. Succinctly, the rate of occurrence of the errors is set to 1.0, meaning that construction errors will occur. In other words, for every run, a deviation to the input of interest is introduced according to the error magnitude model of each construction error, independently. Furthermore, each error magnitude PDF, detrimental or beneficial, is directly linked to a structural failure probability. The results of this analysis are reviewed in the second column of Table 7.

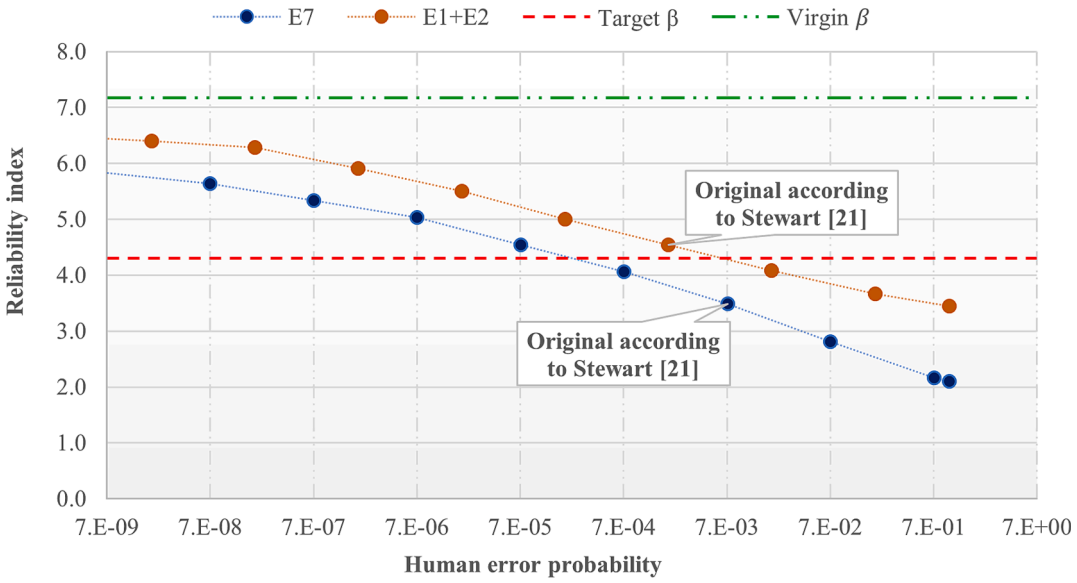

Fig. 8. HEP effect on structural safety.

The beneficial error magnitude PDFs (i.e., E2, E4, E6) had little influence on the structural failure probability, sometimes decreasing the structural reliability slightly. Given the very low initial failure probability of the system, this slight decrease in structural reliability is caused by some inaccuracy or instability in the computation of very low probabilities of failure. One can conclude that the beneficial error models did not improve failure probability in this case study. On the other hand, the detrimental error magnitude PDFs, namely, E1, E5 and E7, significantly impacted the structural failure probability, being E7 the error whose error magnitude PDF had the largest impact on safety reduction.

The error magnitude PDF of E1 (i.e., reduced area of post-tensioning reinforcement) introduced a considerable reduction in structural safety, reducing the initial reliability index from 7.17 to 3.01. With respect to E3, little impact on safety reduction is observed since it was modelled as the effective height of conventional tensile reinforcement; however, the post-tensioning reinforcement is responsible for most of the carrying capacity of the structure. The E5, modelled as width decrease of the different layers of the superstructure's rib, leads to a reliability index of 4.11. Finally, the concrete compressive strength reduction (i.e., E7) was the most detrimental error leading to a reliability index of 1.81, caused mainly by the extension added to the tail of its PDF (see PDF in Fig. 2). Furthermore, the strength reduction affects all layers of the critical cross-sections of the superstructure, i.e., spatial variability of the concrete strength was not considered. Further investigations through random fields are recommended to address this shortcoming.

Despite being carefully defined, the error magnitude PDFs produce values that one may argue as unrealistic or would rarely go undetected and not be mitigated during the construction process—especially those more sensitive to human eyes, i.e., geometry-related errors. For instance, one might find it hard to believe that a complete layer of reinforcement would go missing during the construction of a bridge, which is the case when a realisation with an error magnitude of −100% for E1 (i.e., reduced area of post-tensioning reinforcement) is concerned. Nonetheless, one can also argue that gross errors that sometimes sound unrealistic may have a non-zero likelihood of occurrence [64]. Either way, the range of the values produced by the detrimental error magnitudes PDFs is restricted to more feasible ranges, using bounds displayed in the third column of Table 7. The obtained results considering such constrained PDFs are presented in the last column of Table 7, showing a less significant decrease in structural safety. This was already expected since, with the bounds, the largest deviations previously introduced by the original error magnitude PDFs are removed from the analysis; thus, no significant change to the tail of the original PDF of the random variables affected by the error is introduced. The truncated PDFs still lead to an integral of the distribution equal to one.

6.2. *Detrimental and beneficial errors pairs – HEP and error magnitude PDFs*

Considering now the HRA event tree displayed in Fig. 2, the failure probabilities of the case study are summarised in Table 8 according to the displayed combination of detrimental and beneficial errors. Meaning that the occurrence of either beneficial or detrimental errors is allowed in the probabilistic analysis as described in the HRA event tree in 2.3. The failure probabilities given by the different HEP PDFs (i.e., before and after inspection – see Fig. 1a) differ in one order of magnitude (see Table 8) for the errors concerning the post-tensioning reinforcement area (i.e., E1 + E2) and the superstructure's rib width (i.e., E5 + E6). However, for the concrete compressive strength associated error (i.e., E7), the results are the same since visual inspection works are not expected to have any influence on error detection and, therefore, any influence on the reduction of its HEPs. The models addressing the effective height of the tensile reinforcement (i.e., E3 and E4) have a low impact on safety reduction, as already demonstrated in Table 7 and discussed in 6.1. The concrete compressive strength-related error is identified as the error with the highest impact on safety reduction.

In summary, for a certain range of reduction introduced by the error magnitude PDF to the parameter of interest at a given rate (i.e., number of times $RN_i < HEP_{i,d}$), failure develops into a more likely scenario. For instance, if the strength of the concrete is lower than the required strength to sustain its self-weight and other permanent loads, failure is inevitable since G(X) will assume a negative value. Consequently, the frequency of occurrence of such an event will increase the probability of failure of the structure, especially when the discrepancy between the probability of failure of the error-free scenario and such event is several orders of magnitude.

6.3. *HEP reduction*

The HEP PDFs considered in 6.2 might not adequately mirror today's reality. Considering the latest progress in the quality control and standardisation of the construction process, especially in the bridge engineering field, the decrease of the previously introduced HEPs is a reasonable consideration that should be investigated. Furthermore,

HEPs are also dependent on the skills of the construction worker, internal framework for quality control, socially established frameworks for quality assurance, and risk tolerance, among other factors. As such, scenarios considering the reduction of the HEP are analysed aiming to assess the increase of structural safety due to the decrease of HEPs caused by more effective implementation of quality control strategies. This is accomplished by shifting the mean value of HEP PDFs. Accordingly, Fig. 8 summarises the results of such analysis for the errors with the highest impact on safety reduction, i.e., E1 + E2 and E7.

The increase and decrease of the mean values of the HEP PDFs by one order of magnitude at a time demonstrated a similar trend, for E1 + E2 and E7, in the reduction and increase of safety. Despite not being very evident, one can note a slight tendency for a plateau when the mean values of the HEPs models are approaching the lower end of the chart. Therefore, the impact of construction errors on safety reduction, as modelled in this work, can be constrained if the error rate is ensured to be low enough. Not surprisingly, this is what quality management measures and standards suggest. Meaning, that structural safety can only be assured if efficient quality control measures are in place to constrain the rate of occurrence of errors and by correcting those that have been identified.

The original E7 PDF proposed by Stewart [21] put the structure reliability index below the target safety level, while the original E1 + E2 models put the structural reliability index slightly above the target safety level (see Fig. 8). Nonetheless, from Fig. 8, it is noticeable that the assurance of a structural safety level close to the virgin reliability index (i.e., $\beta = 7.17$) demands a HEP PDF with a mean value way lower than 7.0×10^{-09} for both errors, especially for E7. The virgin reliability index notion, introduced by Hajdin et al. [65,66] and computed in 5.2, refer to the reliability index of the undamaged (i.e., the absence of deterioration process or construction errors) state of the bridge. The results displayed in Fig. 8 suggest that the computed virgin reliability index would be hard to ensure if the construction error models were to be taken into account since, after reduction of the HEPs' mean value in several order of magnitudes, the computed reliability index was still below the virgin reliability index. Furthermore, in real life, a HEP PDF with a mean value below 7.0×10^{-09} seems to be hard to achieve through quality control procedures. One should keep in mind that the analysis is also dependent on the PDFs of the error magnitude and the importance of the parameters affected by them on structural safety.

6.4. Multiple occurrences of detrimental errors

The impact of errors in structural safety should encompass the consideration of the simultaneous occurrence of different errors. Some dependency between the occurrence of different errors is assumed. Such dependency is based on the assumption that one should assume an error-prone realisation for multiple occurrences of errors if a first error has occurred. Therefore, in the HRA event tree, if an error has been recorded is likely that multiple errors (i.e., the simultaneous occurrence of more than one error) will follow in the same realisation. The rate of occurrence of multiple errors and their dependency is provided by the common RN_i used for d^{th} verifications in "Is $RN_i < HEP_{i,d}$?" (see Fig. 2) for different errors. Consequently, for realisations where RN_i takes a very low number, more than one detrimental error is likely to follow because the condition in "Is $RN_i < HEP_{i,d}$?" will likely be true for more than one detrimental error. The simultaneous occurrence of errors was considered most relevant for detrimental errors. This is mainly because beneficial errors were not considered relevant for the improvement of structural safety (see 6.1).

Keeping in mind that there is a maximum of 4 possible detrimental errors per simulation (scenario with results in the last two columns of Table 10), the realisations where one and multiple errors have taken place can be summarised as follow: (i) the rate of occurrence of at least one error is 1.22%, (ii) the rate of occurrence of at least two errors is 0.36%, (iii) the rate of occurrence of at least three errors is 0.076% and (iv) the rate of occurrence of four errors is 0.013%.

Furthermore, as intermediate simulation results, the dependency between two errors is summarised in Table 9. The dependency is here understood as the probability of occurrence of one error given the occurrence of another error (e.g., $P(E_1|E_3)$). Thus, Table 9 should be read as the probability of occurrence of the error in the row given the occurrence of the error in the column. To put the obtained numbers in practical terms, the computed dependency of the errors can be seen as of low, moderate and high dependency if the obtained conditional probabilities are approximately 0.06, 0.15 and 0.51, respectively [67,68].

The impact of multiple errors in structural safety reduction was summarised in Table 10. To assess the influence of the combination of errors in the performance function (i.e., G(X)) for realisations where multiple errors were verified, different surrogates were created for the combinations provided in Table 10. Outputs of the analysis demonstrate that the combination itself did not introduce additional safety reduction since the results show that the probability of failure of the structure is dominated by the most detrimental error in the combination. Simply put, the overall failure probability of the combination will be approximately the failure probability computed for the most detrimental error in the combination. For instance, for combinations where E7 has been introduced, the system failure probability for any combination will be around 2.52×10^{-04} ($\beta = 3.49$). A failure probability that was already obtained in 6.2. Such observation is true because of the difference in the impact of the different errors in the safety reduction.

7. Conclusions

Construction errors are too often neglected when structural safety is concerned. Hence, this work's novelty lies in considering construction errors as an additional source of uncertainty in a surrogate-based structural reliability analysis procedure leading to the quantification of their impact on structural safety reduction. Bearing in mind the assumptions, scenarios, results and the discussion introduced in this work, the following conclusions are drawn:

1. Detrimental and beneficial errors have an asymmetric impact on structural safety. While detrimental errors can decrease structural safety significantly, conservative errors will not increase structural safety considerably. That being said, one needs to state that this does not mean one cannot increase structural safety with strategic decisions.
2. Structural safety levels obtained when neglecting construction errors are hard to assure when construction errors as an additional source of uncertainty are introduced in the analysis, even when human error probabilities are significantly reduced. Simply put, the results suggest that the actual probability of failure of the case study is limited to a certain upper threshold due to construction errors. A system can only be as reliable as the quality control procedure or as good as the efficiency of the error identification and mitigation procedure employed; nonetheless, these can not be improved endlessly.
3. The combination of multiple errors does not reduce the structural safety beyond the safety reduction already introduced by the most detrimental error in the combination. Meaning that, in the end, safety reduction due to construction error can be mostly modelled considering single error occurrence scenarios.

Table 9
Dependency matrix.

	E1	E3	E5	E7
E1	1.00	0.17	0.30	0.14
E3	0.24	1.00	0.35	0.17
E5	0.12	0.10	1.00	0.07
E7	0.56	0.48	0.70	1.00

Table 10
Structural failure probability due to multiple error occurrences.

Two-Errors	Reliability index	Three-Errors	Reliability index	Four-errors	Reliability index
E1 + E3	4.64 (1.76 × 10^{-06})	**E1 + E3 + E5**	4.62 (1.90 × 10^{-06})	**E1 + E3 + E5 + E7**	3.54 (1.98 × 10^{-04})
E1 + E5	3.97 (3.67 × 10^{-05})	**E1 + E3 + E7**	3.56 (1.85 × 10^{-04})		–
E1 + E7	3.52 (2.19 × 10^{-04})	**E1 + E5 + E7**	3.51 (2.22 × 10^{-04})	–	–
E3 + E5	5.85 (2.50 × 10^{-09})	–	–	–	–
E3 + E7	3.52 (2.15 × 10^{-04})	–	–	–	–
E5 + E7	3.50 (2.37 × 10^{-04})	–	–	–	–

The ageing of bridges brings with it a margin of safety reduction and additional uncertainties that must be dealt with. Additionally, execution quality is something infrastructure management institutions and engineers should be concerned with, as well as the compliance of available blueprints with the executed structure back in the day. Therefore, a screening procedure for possible construction errors or construction deficiencies identification is highly recommended when structural safety management is concerned. Furthermore, design errors not addressed in this work should also be investigated despite being part of a more standardised procedure and thus less susceptible to errors.

The combination of construction error models, non-linear FEM and surrogate-based reliability analysis, led to the establishment of relevant benchmark results when construction errors are concerned. Such benchmarks are absent in the literature and are important for an improved understanding of the overall impact of construction errors on the structural safety of bridges.

CRediT authorship contribution statement

Neryvaldo Galvão: Conceptualization, Software, Formal analysis, Investigation, Writing – original draft, Writing – review & editing, Visualization, Project administration, Funding acquisition. **José C. Matos:** Project administration, Resources, Funding acquisition. **Rade Hajdin:** Formal analysis, Writing – review & editing, Supervision, Funding acquisition. **Luís Ferreira:** Resources, Funding acquisition. **Mark G. Stewart:** Resources, Writing – review & editing, Supervision.

Declaration of Competing Interest

The authors declare that they have no known competing financial interests or personal relationships that could have appeared to influence the work reported in this paper.

Acknowledgements

This work is partially financed by (i) national funds through FCT - Foundation for Science and Technology, under grant agreement "PD/BD/143003/2018" attributed to the 1st author; and (ii) FCT / MCTES through national funds (PIDDAC) under the R&D Unit Institute for Sustainability and Innovation in Structural Engineering (ISISE), under reference UIDB / 04029/2020. The authors would also like to acknowledge the Infrastructures of Portugal, in particular the engineer Hugo Patricio, for the support in the identification of a suitable case study and for providing the case study blueprints.

References

[1] International Federation for Structural Concrete (FIB). Model Code for Concrete Structures. Lausanne, Switzerland: Ernst&Sohn; 2010.
[2] European Committee for Standardization (CEN). EN 1990, Eurocode 0: Basis of structural design. Brussels, Belgium: 2002.
[3] Hajdin R, Casas JR, Campos e Matos J. Inspection of Existing Bridges – Moving on from condition rating. IABSE Symp. Towar. a Resilient Built Environ. Risk Asset Manag., Guimarães, Portugal: IABSE; 2019, p. 940–7. https://doi.org/10.2749/guimaraes.2019.0940.
[4] Darmawan MS, Stewart MG. Spatial time-dependent reliability analysis of corroding pretensioned prestressed concrete bridge girders. Struct Saf 2007;29:16–31. https://doi.org/10.1016/j.strusafe.2005.11.002.
[5] Kifokeris D, e Matos JAC, Xenidis Y, Bragança L. Bridge quality appraisal methodology: Application in a reinforced concrete overpass roadway bridge. J Infrastruct Syst 2018;24:04018034. https://doi.org/10.1061/(ASCE)IS.1943-555X.0000455.
[6] Biondini F, Frangopol DM. Time-variant redundancy and failure times of deteriorating concrete structures considering multiple limit states. Struct Infrastruct Eng 2017;13:94–106. https://doi.org/10.1080/15732479.2016.1198403.
[7] Proske D. Estimation of the global health burden of structural collapse. 18th Int. probabilistic work., springer. Nature 2021:327–40. https://doi.org/10.1007/978-3-030-73616-3_24.
[8] Di P. Fatalities due to bridge collapses. Proc Inst Civ Eng Bridg Eng 2020;173:260–7. https://doi.org/10.1680/jbren.20.00001.
[9] Garg RK, Chandra S, Kumar A. Analysis of bridge failures in India from 1977 to 2017. Struct Infrastruct Eng 2020. https://doi.org/10.1080/15732479.2020.1832539.
[10] Schaap HS, Caner A. Bridge collapses in Turkey: causes and remedies. Struct Infrastruct Eng 2020. https://doi.org/10.1080/15732479.2020.1867198.
[11] Wardhana K, Hadipriono FC. Analysis of recent bridge failures in the United States. J Perform Constr Facil 2003;17:144–50. https://doi.org/10.1061/(ASCE)0887-3828(2003)17:3(144).
[12] Syrkov A, Høj NP. Bridge failures analysis as a risk mitigating tool. IABSE Symp. Towar. a Resilient Built Environ. - Risk Asset Manag.: Guimarães, Portugal; 2019. p. 304–10.
[13] Scheer J. Failed bridges - case studies. Causes and Consequences Hannover: Ernst&Sohn 2010. https://doi.org/10.1002/9783433600634.
[14] Galvão N, Matos J, Oliveira DV. Human errors induced risk in reinforced concrete bridge engineering. J Perform Constr Facil 2021. https://doi.org/10.1061/(ASCE)CF.1943-5509.0001595.
[15] Calvi GM, Moratti M, O'Reilly GJ, Scattarreggia N, Monteiro R, Malomo D, et al. Once upon a time in italy: the tale of the morandi bridge. Struct Eng Int 2019;29:198–217. https://doi.org/10.1080/10168664.2018.1558033.
[16] Malomo D, Scattarreggia N, Orgnoni A, Pinho R, Moratti M, Calvi GM. Numerical study on the collapse of the morandi bridge. J Perform Constr Facil 2020;34:04020044. https://doi.org/10.1061/(asce)cf.1943-5509.0001428.
[17] Pujol S, Kreger ME, Monical JD, Schultz AE. Investigation of the Collapse of the Chirajara. Concr Int 2019;41:29–37.
[18] Peng W, Tang Z, Wang D, Cao X, Dai F, Taciroglu E. A forensic investigation of the Xiaoshan ramp bridge collapse. Eng Struct 2020;224. https://doi.org/10.1016/j.engstruct.2020.111203.
[19] Proske D. Bridge Collapse Frequencies versus Failure Probabilities. Cham: Springer International Publishing; 2018. https://doi.org/10.1007/978-3-319-73833-8.
[20] Lind NC. Models of human error in structural reliability. Struct Saf 1982;1:167–75. https://doi.org/10.1016/0167-4730(82)90023-6.
[21] Stewart MG. A human reliability analysis of reinforced concrete beam construction. Civ Eng Syst 1992;9:227–50. https://doi.org/10.1080/02630259208970651.
[22] Stewart MG. Modeling human performance in reinforced concrete beam construction. J Constr Eng Manag 1993;119:6–22. https://doi.org/10.1061/(asce)0733-9364(1993)119:1(6).
[23] Swain AD, Guttmann HE. Handbook of reliability analysis with emphasis on nuclear plant applications. Washington, D.C.: 1983.
[24] Stewart M, Melchers R. Error control in member design. Struct Saf 1989;6:11–24. https://doi.org/10.1016/0167-4730(89)90004-0.
[25] Stewart M. Structural reliability and error control in reinforced concrete design and construction. Struct Saf 1993;12:277–92. https://doi.org/10.1016/0167-4730(93)90057-8.
[26] Stewart MG. Human error in steel beam design. Civ Eng Syst 1990;7:94–101. https://doi.org/10.1080/02630259008970576.
[27] Stewart MG, Melchers RE. Decision model for overview checking of engineering designs. Int J Ind Ergon 1989;4:19–27. https://doi.org/10.1016/0169-8141(89)90046-2.
[28] Epaarachchi DC, Stewart MG. Human error and reliability of multistory reinforced-concrete building construction. J Perform Constr Facil 2004;18:12–20. https://doi.org/10.1061/(ASCE)0887-3828(2004)18:1(12).
[29] Bhattacharyya B. Uncertainty quantification and reliability analysis by an adaptive sparse Bayesian inference based PCE model. Eng Comput 2021;1:3. https://doi.org/10.1007/s00366-021-01291-0.
[30] Teixeira R, Martinez-Pastor B, Nogal M, O'Connor A. Reliability analysis using a multi-metamodel complement-basis approach. Reliab Eng Syst Saf 2020;107248. https://doi.org/10.1016/j.ress.2020.107248.
[31] Teixeira R, Nogal M, O'Connor A. Adaptive approaches in metamodel-based reliability analysis: a review. Struct Saf 2021;89. https://doi.org/10.1016/j.strusafe.2020.102019.
[32] Lataniotis C, Wicaksono D, Marelli S, Sudret B. UQLab user manual - Kriging (Gaussian process modeling), Report # UQLab-V1.4-105. Zurich, Switzerland: 2021.

[33] Echard B, Gayton N, Lemaire M. AK-MCS: an active learning reliability method combining Kriging and Monte Carlo Simulation. Struct Saf 2011;33:145–54. https://doi.org/10.1016/j.strusafe.2011.01.002.
[34] M. Moustapha, S. Marelli and BS. UQLab user manual - Active learning reliability, Report UQLab-V1.4-117. Zurich, Switzerland: 2021.
[35] Marelli S, Sudret B. An active-learning algorithm that combines sparse polynomial chaos expansions and bootstrap for structural reliability analysis. Struct Saf 2018; 75:67–74. https://doi.org/10.1016/j.strusafe.2018.06.003.
[36] Marelli S, Schobi R, Sudret B. UQLab user manual - Structural Reliability (Rare Event Estimation), Report # UQLab-V1.4-107. Zurich, Switzerland: 2021.
[37] Schneider R, Thöns S, Straub D. Reliability analysis and updating of deteriorating systems with subset simulation. Struct Saf 2017;64:20–36. https://doi.org/10.1016/j.strusafe.2016.09.002.
[38] European Committee for Standardization (CEN). EN 1991-2, Eurocode 1: Actions on structures - Part 2: Traffic loads on bridges. Brussels, Belgium: 2003.
[39] de Portugal I. Case study II blue prints (Internal Reference). Portugal: Lisboa; 2006.
[40] Diana TNO. User's manual - material library. release 10. Delft, The Netherlands: TNO DIANA bv; 2020.
[41] TNO DIANA. User's Manual - Element Library. Release 10. Delft, The Netherlands: 2020.
[42] TNO DIANA. User ' s Manual - Analysis Procedures. Release 10. Delft, The Netherlands: TNO DIANA bv; 2020.
[43] Hendriks MAN, de Boer A, Belletti B. Guidelines for nonlinear finite element analysis of concrete structures - RTD:1016-1:2017. 2017.
[44] European Committee for Standardization (CEN). EN 1992-1-1, Eurocode 2: Design of concrete structures - Part 1-1: General rules and rules for buildings. Brussels, Belgium: 2004.
[45] Wisniewski DF, Casas JR, Ghosn M. Simplified probabilistic non-linear assessment of existing railway bridges. Struct Infrastruct Eng 2009;5:439–53. https://doi.org/10.1080/15732470701639906.
[46] Wiśniewski DF, Cruz PJS, Henriques AAR, Simões RAD. Probabilistic models for mechanical properties of concrete, reinforcing steel and pre-stressing steel. Struct Infrastruct Eng 2012;8:111–23. https://doi.org/10.1080/15732470903363164.
[47] Casas JR, Wisniewski D. Safety requirements and probabilistic models of resistance in the assessment of existing railway bridges. Struct Infrastruct Eng 2013;9: 529–45. https://doi.org/10.1080/15732479.2011.581673.
[48] Joint Committee on Structural Safety (JCSS). Probabilistic Model Code - Part 3: Material properties. 2000.
[49] Wisniewski D, Casas JR, Henriques AA, Cruz PJS. Probability-based assessment of existing concrete bridges-stochastic resistance models and applications. Struct Eng Int J Int Assoc Bridg Struct Eng 2009;19:203–10. https://doi.org/10.2749/101686609788220268.
[50] Danish Road Directorate. Reliability-based classification of the load carrying capacity of existing bridges. Denmark: Danish Road Directorate (DRD); 2004.
[51] O'Connor A, Pedersen C, Gustavsson L, Enevoldsen I. Probability-based assessment and optimised maintenance management of a large riveted truss railway bridge. Struct Eng Int 2009;19:375–82. https://doi.org/10.2749/101686609789847136.
[52] Honfi D, Mårtensson A, Thelandersson S. Reliability of beams according to Eurocodes in serviceability limit state. Eng Struct 2012;35:48–54. https://doi.org/10.1016/j.engstruct.2011.11.003.
[53] Moreira VN, Matos JC, Oliveira DV. Probabilistic-based assessment of a masonry arch bridge considering inferential procedures. Eng Struct 2017;134:61–73. https://doi.org/10.1016/j.engstruct.2016.11.067.
[54] European Committee for Standardization (CEN). EN 1992-2, Eurocode 2: Design of concrete structures - Part 2: Concrete bridges - Design and detailing rules. Brussels, Belgium: 2005.
[55] (CEN) EC for S. EN 13670, Execution of concrete structures. Brussels, Belgium: 2007.
[56] Moustapha M, Marelli S, Sudret B. UQLab user manual – The UQLINK module, Report #UQLab-V1.4-110. Zurich, Switzerland: 2021.
[57] Lataniotis C, Torre E, Marelli S, Sudret B. UQLab user manual – The Input module, Report # UQLab-V1.4-102. Zurich, Switzerland: 2021.
[58] Galvão N, Matos JC, Oliveira DV, Hajdin R. Human error impact in structural safety of a reinforced concrete bridge. Struct Infrastruct Eng 2021:1–15. https://doi.org/10.1080/15732479.2021.1876105.
[59] Matos JC, Moreira VN, Valente IB, Cruz PJS, Neves LC, Galvão N. Probabilistic-based assessment of existing steel-concrete composite bridges – application to sousa river bridge. Eng Struct 2019;181:95–110. https://doi.org/10.1016/j.engstruct.2018.12.006.
[60] Blatman G, Sudret B. Adaptive sparse polynomial chaos expansion based on least angle regression. J Comput Phys 2011;230:2345–67. https://doi.org/10.1016/j.jcp.2010.12.021.
[61] Ghasemi SH, Nowak AS. Target reliability for bridges with consideration of ultimate limit state. Eng Struct 2017;152:226–37. https://doi.org/10.1016/j.engstruct.2017.09.012.
[62] Sykora M, Diamantidis D, Holicky M, Jung K. Target reliability for existing structures considering economic and societal aspects. Struct Infrastruct Eng 2017; 13:181–94. https://doi.org/10.1080/15732479.2016.1198394.
[63] Lataniotis C, Marelli S, Sudret B. UQLab user manual – the model module. Switzerland: Zurich; 2021.
[64] Fröderberg M, Thelandersson S. Uncertainty caused variability in preliminary structural design of buildings. Struct Saf 2014;52:183–93. https://doi.org/10.1016/j.strusafe.2014.02.001.
[65] Hajdin R, Kusar M, Masovic S, Linneberg P, Amado J, Tanasić N. Establishment of quality control plan - Cost Action TU1406. 2018. https://doi.org/10.13140/RG.2.2.28730.03526.
[66] Hajdin R. Managing existing bridges - on the brink of an exciting future. Maintenance, Safety, Risk. Manag Life-Cycle Perform Bridg - Proc 9th Int Conf Bridg Maintenance, Saf Manag IABMAS 2018, 2018..
[67] Stewart MG, Ginger JD, Henderson DJ, Ryan PC. Fragility and climate impact assessment of contemporary housing roof sheeting failure due to extreme wind. Eng Struct 2018;171:464–75. https://doi.org/10.1016/j.engstruct.2018.05.125.
[68] Kirwin B. A guide to practical human reliability assessment. London, UK: Taylor & Francis; 1994.